



HAL
open science

Modelling of drainage dynamics influence on sediment routing system in a fold-and-thrust belt

Marc Viaplana-Muzas, Julien Babault, Stephane Dominguez, Jean van den Driessche, Xavier Legrand

► **To cite this version:**

Marc Viaplana-Muzas, Julien Babault, Stephane Dominguez, Jean van den Driessche, Xavier Legrand. Modelling of drainage dynamics influence on sediment routing system in a fold-and-thrust belt. Basin Research, 2019, 31 (2), pp.290-310. 10.1111/bre.12321 . insu-01983103

HAL Id: insu-01983103

<https://insu.hal.science/insu-01983103>

Submitted on 8 Feb 2024

HAL is a multi-disciplinary open access archive for the deposit and dissemination of scientific research documents, whether they are published or not. The documents may come from teaching and research institutions in France or abroad, or from public or private research centers.

L'archive ouverte pluridisciplinaire **HAL**, est destinée au dépôt et à la diffusion de documents scientifiques de niveau recherche, publiés ou non, émanant des établissements d'enseignement et de recherche français ou étrangers, des laboratoires publics ou privés.

DR MARC VIAPLANA-MUZAS (Orcid ID : 0000-0003-4175-8339)

Article type : Original Article

Modeling of drainage dynamics influence on sediment routing system in a fold-and-thrust belt

Marc Viaplana-Muzas^a, Julien Babault^b, Stéphane Dominguez^c, Jean Van Den Driessche^d, Xavier Legrand^e

^a Group of Dynamics of the Lithosphere (GDL), Institute of Earth Sciences Jaume Almera (ICTJA-CSIC), Lluís Solé i Sabarís s/n, 08028 Barcelona, Spain.

mviaplana@ictja.csic.es; marc.via.mu@gmail.com

^b LFCR, Université de Pau et des Pays de l'Adour, 64013 Pau Cedex, France,

now at: Instituto Geológico y Minero de España, 28760 Tres Cantos, Madrid, Spain

ju.babault@gmail.com

^c Université de Montpellier, Géosciences Montpellier, F-34095, Montpellier, France.

dominguez@gm.univ-montp2.fr

^d Géosciences Rennes, Université de Rennes 1, Campus de Beaulieu, Rennes, France.

jean.van-den-driessche@univ-rennes1.fr

^e Petronas CariGali, Twin Tower KLCC, 50088, Kuala Lumpur, Malaysia.

legrand.xavier@petronas.com.my

This article has been accepted for publication and undergone full peer review but has not been through the copyediting, typesetting, pagination and proofreading process, which may lead to differences between this version and the Version of Record. Please cite this article as doi: 10.1111/bre.12321

This article is protected by copyright. All rights reserved.

Abstract

Drainage networks link erosional landscapes and sedimentary basins in a source-to-sink system, controlling the spatial and temporal distribution of sediment flux at the outlets. Variations of accumulation rates in a sedimentary basin have been classically interpreted as changes in erosion rates driven by tectonics and/or climate. We studied the interactions between deformation, rainfall rate and the intrinsic dynamics of drainage basins in an experimental fold-and-thrust belt subjected to erosion and sedimentation under constant rainfall and shortening rates. The emergence of thrust sheets at the front of a prism may divert antecedent transverse channels (perpendicular to the structural grain) leading to the formation of longitudinal reaches, later uplifted and incorporated in the prism by the ongoing deformation. In the experiments, transverse incisions appear in the external slopes of the emerging thrust sheets. Headward erosion in these transverse channels results in divide migration and capture of the uplifted longitudinal channels located in the inner parts of the prism, leading to drainage network reorganization and modification of the sediment routing system. We show that the rate of drainage reorganization increases with the rainfall rate. It also increases in a non-linear way with the rate of uplift. We explain this behavior by an exponent >1 on the slope variable in the framework of the stream power erosion model. Our results confirm the view that early longitudinal-dominated networks are progressively replaced by transverse-dominated rivers during mountain building. We show that drainage network dynamics modulate the distribution of sedimentary fluxes at the outlets of experimental wedges. We propose that under constant shortening and rainfall rates the drainage network reorganization can also modulate the composition and the spatial distribution of clastic fluxes in foreland basins.

Keywords: drainage network dynamics, source-to-sink system, sedimentary flux, sediment accumulation rates, experimental modeling, fold-and-thrust belt, headward erosion, capture, divide migration, foreland basins.

Introduction

The main agent responsible for erosion and transport of sediment is the drainage network which links erosional and depositional landscapes in a source-to-sink system (Meade, 1982; Leeder, 1997). The flux of sediments transported by rivers is controlled by erosion rates in the source areas and determines sedimentation rates in fluvial outlets feeding the sink. Fluvial erosion in mountain ranges is often approximated by the stream power law (Howard & Kerby, 1983) stating that erosion is proportional to discharge and river slope, hence governed by climate and tectonics (Howard, 1967; Peizhen *et al.*, 2001; Whipple, 2001). Tectonics also controls the drainage network organization which, by the location of its main outlets, rules the spatial distribution of the clastic bodies and the patterns of sedimentation in the basins (Gupta, 1997; Horton & DeCelles, 2001; Viaplana-Muzas *et al.*, 2015). The best examples are in fold-and-thrust belts where rivers may be deviated by emerging thrusts, causing trellis drainage patterns to form where longitudinal rivers flow parallel to the structural grain (Jackson *et al.*, 1996; Gupta, 1997; van der Beek *et al.*, 2002; Viaplana-Muzas *et al.*, 2015). The erosion capacity of antecedent transverse channels to overcome the uplift on a thrust

Accepted Article

sheet depends on its discharge (e.g., Burbank *et al.*, 1999; Tomkin & Braun, 1999) and experiments suggest that the minimum discharge needed increases non-linearly with uplift rate (Viaplana-Muzas *et al.*, 2015). However, the drainage organization within a mountain range is traditionally assumed to follow the regional slope with rivers flowing from the main divide toward the front of deformation (Hovius, 1996; Talling *et al.*, 1997) resulting in a transverse-dominated drainage network, perpendicular to the structural grain, with drainage boundaries considered to be static. This view was reinforced by numerical modeling of erosion in uplifting landscapes (Tucker & Slingerland, 1994; Crave & Davy, 2001; Willett *et al.*, 2001) and by experimental modeling (Bonnet & Crave, 2003; Babault *et al.*, 2005). Therefore changes in clastic sedimentary flux, grain size and provenance in clastic sediments are classically interpreted as variations of erosion rates driven by tectonics and/or climate (e.g., Leeder *et al.*, 1998; Peizhen *et al.*, 2001; Armitage *et al.*, 2011).

However, recent works show that the boundaries of the drainage basins are modified by drainage divide migration and river capture during mountain building (Bishop, 1995; Willett *et al.*, 2001; Pelletier, 2004; Bonnet, 2009; Babault *et al.*, 2012; Perron *et al.*, 2012; Goren *et al.*, 2014) and by deformation of the lithosphere (e.g., Hallet & Molnar, 2001; Castelltort *et al.*, 2012). The impact of drainage dynamics on erosion rates and river longitudinal profile evolution may be of second order when compared to rock uplift, because rivers adapt faster to drainage reorganization-induced changes in downstream slopes than divide migration rates (Whipple *et al.*, 2017). In two sided orogens eroded by transverse rivers, captures involve small low-order streams and reorganization is dominated by continuous divide migration during tens of millions of years (e.g., Willett *et al.*, 2001; Fox *et al.*, 2014; Goren *et al.*, 2014; Willett *et al.*, 2014; Whipple *et al.*, 2017). However, numerical models show that in cases where rivers flowing in one direction are replaced by rivers perpendicular to them, captures of larger rivers can occur (Whipple *et al.*, 2017). During mountain building, a drainage network may evolve from an early stage characterized by the presence of thrust controlled, longitudinal dominant channels parallel to the main structures, to transverse dominant channels perpendicular to the main structures (e.g., Babault *et al.*, 2018, and references therein). This macroscale reorganization of drainage network, triggered by a systematic process of drainage divide migration, potentially implies capture events of large drainage areas which in turn may modify the sediment routing system, the spatial distribution of erosion, and the amounts and provenance of clastic sediments (Bishop, 1995). Consequently, drainage networks, combined with tectonics and climate, may control the sedimentary architecture in foreland basins. The dynamics of topography during the building of accretionary wedges has recently been reproduced in 3D numerical models (Ueda *et al.*, 2015). But to date there is no systematic analysis in accretionary prisms of drainage network dynamics and its related patterns of sedimentation.

In this study, we investigate experimentally the impact of drainage reorganization from longitudinal- to transverse-dominated network on sedimentation by a detailed geomorphic and stratigraphic analysis of experimental accretionary prisms. We perform new analyses of the models previously presented in Viaplana-Muzas *et al.* (2015), who focused on how shortening, uplift and rainfall rates control the early development of longitudinal channels during the emergence of thrust sheets (early drainage organization). Here, we investigate under temporally constant shortening and rainfall rates

the factors controlling drainage divide dynamics, between early longitudinal channels and expanding transverse channels, by varying systematically the shortening and rainfall rates. We further document the relationships between drainage divide migration, captures, intensity of erosion and sediment supply in front of the experimental wedges. We finally compare our experimental results to natural systems.

1. Method

1.1. Setup

The experiments run in a sand-box type 3D experimental device (0.8 m × 2.4 m) which allows the study of the interactions between tectonics, erosion and sedimentation in accretionary prisms subjected to rainfall (Graveleau & Dominguez, 2008; Graveleau *et al.*, 2012; Graveleau *et al.*, 2015; Viaplana-Muzas *et al.*, 2015). Deformation is induced by pulling a basal film beneath a static buttress (backstop), resulting in a wedge created by imbricate thrust sheets that emerge at the forefront (Fig. 1). Deformation propagates in sequence with minor thrust reactivation (Animation 3 in Supplementary data, lateral view of exp. A2). Surface processes are modeled by delivering micro-droplets (diameter $\leq 100 \mu\text{m}$), in sequences of 10 seconds with rain and 3 seconds without rain, over the model. The sequence rain/no rain is implemented to limit channel widening induced by high channel flow dynamics (Viaplana-Muzas *et al.*, 2015). We use two different analogue materials: material IV and material 50-50 (“*Mat. IV*” and “*Mat. 50-50*” in Fig.1A). The upper layer consists of glass microbeads, 46%, silica powder, 30% and plastic powder (PVC), 24% (material IV). The lower layer consists of glass microbeads and PVC in equal proportion (material 50-50). We add a basal 5 mm layer of glass microbeads as a décollement layer. Another thin layer of glass microbeads is deposited in the middle of the material IV in order to allow the slip between “*Mat. IV*” layers resulting in folding above thrust ramps. The total thickness is set at 55 mm in order to produce ~ 14 cm spaced thrust sheets. This spacing avoids the burial of the frontal emerging thrust sheet by the sedimentary fans allowing the formation of longitudinal reaches. We reduce the friction on the walls for folds to be cylindrical and thrust sheets to be linear. This is achieved by applying a lubricant on the walls of the sandbox before filling up with the erosion material.

The erosion law in the models can be approximated by the stream power law of the form (e.g., Howard & Kerby, 1983; Whittaker *et al.*, 2007):

$$E = K \cdot \frac{A^m}{W} \cdot S^n \quad \text{eq. 1,}$$

where the exponents m and n are 0.8 ± 0.2 and 1.5 ± 0.2 , respectively (Viaplana-Muzas *et al.*, 2015), A is drainage area (as a proxy for catchment discharge), W is channel width, and S is downstream channel slope.

In this work, we analyze five experiments run under a rainfall rate of 9 mm/h and under shortening rates ranging between 8 cm/h to 100 cm/h (series A, Table 1), and two experiments run under a two-fold higher rainfall rate of 18 mm/h, and at shortening rates of 8 cm/h and 18 cm/h (series B, Table 1). In all the experiments shortening rate and rainfall rate are held constant.

Digital Elevation Models (DEM) of the experiments are acquired using an optical measurement device composed by high resolution cameras coupled to a laser interferometer. The DEM resolution is close to 0.2 mm. The acquisition of each DEM requires to stop both shortening and rainfall systems (during 30-45 min) in order to dry the uppermost 1-2 mm of the model surface and avoid distortions in the brightness of the laser that could affect DEM resolution. In order to study the evolution of the relief three photograph cameras are situated in the lateral, bottom and oblique to the experiment (Graveleau & Dominguez, 2008). Finally, when the experiment is partially dried (one week after the end of the experiment), we cut the model in serial cross-sections in order to study the geometry of thrusts and syntectonic deposits.

1.2. Quantification of the celerity of headward erosion and drainage reorganization response time

In order to measure the rate of drainage network reorganization triggered by the transverse channels, we calculate the celerity of headward erosion in the headwaters of the expanding transverse channels incising the external part of the emerging thrust sheets. We first measure the distance between the trace of a thrust sheet and the headwater of a transverse channel. We divide these measures by the time of activity of a thrust sheet, i.e. the time between its emergence and the emergence of a new one. Distances are measured using the tool "Point Distance" of the software ArcGis. The algorithm extracts the shorter distance between the points that define the headwaters of the transverse channels and the trace of the frontal thrust. The values of celerity of the divide migration and their standard deviations are calculated using the mean and standard deviation of the distances measured with the "Point Distance" tool. We study the headward erosion of all the transverse channels developing in the external limb of all the thrust sheets that appear in each experiment. We use the average distance of headward erosion and its duration to calculate the mean celerity of divide migration above each thrust sheet in each experiment. We calculate the drainage reorganization response time above each thrust sheet dividing the distance between longitudinal channels located in the hanging walls and the trace of the thrusts by the divide migration celerity measured in the experiments. The values of drainage reorganization response time and their standard deviations are the result of averaging these distances. We limit our analysis to thrust sheets large enough to prevent drainage network reorganization (longitudinal to transverse channels) by sedimentary overfilling of the back limbs of the thrust sheets. We therefore discard thrust sheets which present several sub-thrust sheets. We also discard thrust sheets where landslide processes are responsible for erosion and drainage expansion in the external part of the emerging thrust sheets to focus on fluvial erosion.

1.3. Quantification of eroded volumes, and incision, erosion and uplift rates

The amounts of erosion, incision and uplift in the experiments are estimated by subtracting the incised topography from the uplifted and uneroded topographies, which are reconstructed using a rectangular-moving window (1x80 mm). The width of the window, perpendicular to the transverse-channel, is determined by the widest valleys. The 1 mm length side of the moving window, parallel to the transverse channels, is set to take into account the folding of the deformed topography. The reconstructed topographies are derived by extracting the highest values of the rectangular-moving window (Viaplana-Muzas *et al.*, 2015). For each thrust sheet, we calculate the average incision from the depth of incision below the reconstructed topographies along the downstream profiles of all the transverse channels but the antecedent transverse channels. Sub-thrust sheets are not included in this analysis.

1.4. Quantification of the slope of the transverse channels

We measure downstream slopes along the expanding transverse channels using the GridVisual program (P. Davy, University of Rennes 1, <http://terrasse.geosciences.univrennes1.fr/?p=1>) and they are averaged for each analyzed thrust sheet. We use the mean downstream slopes and standard deviations.

1.5. Quantification of sedimentation rates

We calculate the accumulation rates in the sedimentary fans located in front of the external thrusts at the outlet of transverse channels using colored layers made by tinted analogue material sprinkled on the sedimentary fans. We sprinkle dry material tinted in green before any capture and in red after. Markers are systematically added after phases of digitalization of the topographic surfaces. After drying of the experiments, we cut the experiments and the colored layers are used as “timelines”, allowing us to calculate sedimentation rates. The thickness of sediments is measured in between the colored layers. These values are maximum values of sedimentation rate because the cross-sections pass through the middle of the fans where the fan thicknesses are the highest.

1.6. Dimensionless time (T^*)

In order to allow a time extrapolation of the surface processes in our models to nature, we calculate a dimensionless time, T^* . We normalize the time in models by a reference time, defined as the time needed to shorten the system by the same amount as the thickness of the undeformed material that enters into the accretionary wedge (55 mm). We later refer to both, the time in the models and the dimensionless time, and the timing of captures is given by the difference between the T^* of the emergence of a thrust sheet and the T^* at which a capture occurs above that thrust (ΔT^*).

2. Results

2.1. Erosive processes near the divides

Small transverse channels incise into the external part of a thrust sheet as it emerges (e.g., the trace of the thrust sheets in experiments A3 and B1, Figs. 2A and 2C and Animation 1 in Supplementary data). These small transverse channels are the downstream parts of preexisting transverse flows that are separated from their upstream channel by diversion in response to uplift. In Figs. 2B and 2D we see that ongoing erosion in these small transverse channels leads to the migration of their headwaters towards the inner part of the thrust sheets, above which flow longitudinal reaches that gather the upstream areas from the beheaded catchments. Headward erosion in the external transverse channels occurs in amphitheater-headed channels. For example, we observe water emergence in the shallower layer of the experimental material, in the first millimeter below the topographic surface, indicating some water infiltration. However, channels in the headwaters incise several millimeters into the uplifting thrust sheets in series A experiments (Figs. 2A and 2B), indicating that even if headward erosion is the result of the combination of both sapping and channelized flows, seepage erosion is not the dominant process for headward erosion (Figs. 2A and 2B). In the experiments of series B subjected to a higher rainfall rate, amphitheater-headed channels are larger and deeper suggesting a higher influence of seepage erosion on headward erosion (Fig. 2D). In the experiment run under the highest shortening rates, high local slopes develop in front of the thrusts and liquefaction of the material occurs, producing landslides and debris flows. Headward erosion resulting from landslide events has been discarded in our analysis to focus on channels erosion by fluvial processes.

2.2. Divide migration and captures

We observe drainage reorganization by captures of longitudinal channels by transverse 1 in two of the experiments of series A, run under a rainfall rate of 9 mm/h and at shortening rates of 8 cm/h (A2, Table 1, Fig. 3, from A to F, and Fig. SD1) and 9 cm/h (A3, Table 1, Fig. 4, from A to F and Fig. SD2), respectively, and in one of series B, run under a rainfall rate of 18 mm/h and at a shortening rate of 8 cm/h (B1, Table 1, Fig. 5, from A to H and Fig. SD3). In the experiments A3 and B1, 60 cm and 30 cm respectively of shortening occurs after the captures. Post depositional deformation of the eroded products fed by the captured and captor channels prevents any detailed study of the influence of drainage reorganization on sedimentary fluxes in these two experiments (e.g., Fig. 5H). In the case of the experiment A2, we stop the experiment after a few centimeters of shortening following the capture to study the influence of drainage reorganization from a longitudinal- to a transverse-dominated drainage on sedimentary fluxes.

In these three experiments, we observe a similar pattern of evolution of the drainage network that we divide into four main stages. First, when a new thrust sheet starts to emerge the preexisting transverse channels start to incise the uplifting topography (Fig. 3A at $T^* = 8.1$, Fig. 4A at $T^* = 5.0$ and Figs. 5A and 5E at $T^* = 3.6$ and $T^* = 5.2$, respectively). Second, ongoing uplift deflects the smallest transverse channels resulting in the formation of longitudinal reaches in the backlimb of the thrust

Accepted Article

sheet. The longitudinal reaches gather the upstream areas from the beheaded transverse channels (Fig. 3B at $T^* = 8.7$, Fig. 4B at $T^* = 5.3$ and Fig. 5B at $T^* = 4.1$). Some of the preexisting transverse channels integrate the drainage areas gathered by the longitudinal reaches, therefore increasing sufficiently their discharge to cross-cut the uplifting thrust sheets (persistent transverse channels in Viaplana-Muzas *et al.*, 2015). The products of erosion of the persistent transverse channels accumulate at the front of the thrust sheets forming sedimentary fans (F1 and F3 in Fig. 3B, F1 in Fig. 4B and F1 and F4 in Figs. 5B and 5F, respectively). Sedimentation is almost negligible where the thrusts act as topographic barriers, in the zone located between the outlets of the persistent transverse channels and their associated sedimentary fans. Third, the increase of local slopes related to uplift on the frontal thrusts triggers (i) the incision of transverse channels in the forelimb of the thrust sheet and (ii) the divide migration by headward erosion towards the inner part of the wedge, where the longitudinal reaches are located (Fig. 3B at $T^* = 8.7$, Fig. 4C at $T^* = 5.6$ and and Figs. 5C and 5F at $T^* = 4.3$ and $T^* = 6.2$, respectively). Fourth, as soon as the headwaters of a transverse channel reach the bed of a longitudinal channel, it causes the capture of the latter and of its source area, resulting in an elbow of capture over the thrust sheet. Post capture incision waves migrate upstream in the transverse captor reaches (ex., Fig. 3E at $T^* = 10.4$). In the experiment A2, a first capture occurs at $\Delta T^* = 1.6$ (Fig. 3C) followed by two captures at $\Delta T^* = 1.9$ (Fig. 3D) and $\Delta T^* = 2.9$ (Fig. 3F), respectively, in response to the propagation of a wave of incision triggered by the first capture. In the experiment A3, a capture occurs at $\Delta T^* = 1.4$ (Fig. 4D). In the experiment B1, two captures occurred simultaneously at $\Delta T^* = 1.0$ (Fig. 5D) on the thrust sheet nº 3, and another one on the thrust sheet nº4 at $\Delta T^* = 2.1$ (Fig. 5G). Captures result in the formation of new sedimentary fans at the front of the accretionary wedges, in areas of low sedimentation rates before the capture events. In the experiment A2, we observe an increase of the size of the fan F2 following each capture. The fans fed by the captors can reach sizes comparable to those of the fans fed by the persistent transverse channels (ex. Figs. 3E and 5E).

2.3. Divide migration celerity

Accepted Article

For all experiments, we measure the celerity of channel head propagation in the transverse channels located in the external limb of the thrust sheet (as in Fig. 2) to monitor dynamics of the drainage divides that separate the external transverse channels from the longitudinal reaches confined above the thrust sheets. Fig. 6 shows the mean celerity of divide migration in each thrust sheet as a function of the corresponding mean uplift rate (U). In the experiments run under a rainfall rate of 9 mm/h (series A experiments), the divide migration velocity increases with uplift rate from 0.3 mm/min in the experiment A2 to 3.7 mm/min in the model A6 ($C_A = 1.47 \times U^{0.85}$). In the models run under a rainfall rate of 18 mm/h (series B experiments), the divide migration celerity also increases with uplift rate, from 0.7 mm/min in the experiment B1 to 1.2 mm/min in the model B2. In series B experiments, divide migration velocities are almost two-fold higher with respect to that of series A models ($C_B = 2.31 \times U^{0.85}$). In this later regression analysis, we fix the value of the exponent on U at 0.85, following the better constrained exponent on U obtained for series A in which uplift rates cover one order of magnitude (Fig. 6).

2.4. Controls on the celerity of divide migration

We have shown that a positive relationship relates the celerity of divide migration (C) with relative uplift rate (U) of the growing thrust sheets. Analytical and numerical analyses of divide migration rate in the framework of the stream power law also predict a positive relationship between divide migration and relative uplift rate when the exponent n on slope in the stream power erosion law (eq. 1) is >1 (Whipple *et al.*, 2017). This is consistent with our experiments where $n = 1.5$ (Viplana-Muzas *et al.*, 2015). Our results also indicate that drainage reorganization is faster in more humid conditions (Fig. 6). This is consistent with analytical and numerical analyses which also show a positive correlation between divide migration rate and material erodibility, K , in the stream power erosion law (Whipple *et al.*, 2017). We can explain this relation by expressing C as a simple function of the mean vertical incision ($\langle I \rangle$) into the uplifting thrust sheet resulting from the expansion of the transverse channels of mean downstream gradient ($\langle S \rangle$). Let us assume that (i) uplift rate is constant and spatially homogenous above the thrust ramp, (ii) the small transverse channels that incise the uplift have a constant downstream gradient along their long profile, and (iii) erosion is negligible in the longitudinal reach passively transported on top of the hanging wall of a thrust. We determine from the geometry of Fig. 7A that the predicted celerity of divide migration has the form:

$$C_{pred} = \frac{2 \langle I \rangle}{\langle S \rangle} \quad \text{eq. 2,}$$

The second assumption is justified by the very low concavity in the transverse channels. The third assumption is satisfied in the experiments where we observe smooth surfaces preserved from incision (Fig. 2). The mean incision rate ($\langle I \rangle$) in the uplifting thrust sheet and the mean downstream slopes ($\langle S \rangle$) in the expanding transverse channels are both measurable in the experiments.

For series A, we calculated the function linking C_{pred} and uplift rate by examining the relationships between $\langle I \rangle$ and U , and $\langle S \rangle$ and U . We observed that the mean incision rate increases almost linearly with uplift rate (Fig. 7B):

$$\langle I \rangle = 0.29U^{1.11 \pm 0.09} \quad \text{eq. 3,}$$

Channel gradients are dynamically controlled by the competition between uplift and erosion and we observe a concave down increase of mean channel slopes S with uplift rate U (Fig. 7C):

$$\langle S \rangle = 0.45U^{0.29 \pm 0.05} \quad \text{eq. 4,}$$

This behavior is expected to depend on the exponent n on slope in the erosion law (eq. 1), the higher the value of n , the smaller the exponent in eq. 4 (Whipple & Tucker, 1999; Snyder *et al.*, 2000; Lague, 2014). Values of $n > 1$ can explain the weak dependence of channel gradients on the uplift rate. We replaced the equations 3 and 4 in 2 to obtain:

$$C_{pred} = a U^b \quad \text{eq. 5,}$$

with $a = 1.27$ and $b \approx 0.82$ in series A (Fig. 6). Only 5 thrust sheets have been studied in series B and the regression of $\langle I \rangle$ and $\langle S \rangle$ versus uplift rate (red lines in Figs. 7D and 7E) predict values of C_{pred} different than those we observe. More experiments with a wider range of uplift rate would be required to better constrain these relations as observed in series A. Instead, we propose two acceptable regressions within 95% confidence envelopes (dashed lines in Figs. 7D and 7E) that predict

a good fit of C_{pred} vs. $C_{observed}$ when replaced in eq. 5, with $a = 2.16$ and $b = 0.85$ (Fig. 6). In series A, the predicted divide migration velocities C_{Apred} slightly underestimate the observed divide migration celerity. The uneven spatial distribution of uplift above the slightly concave-up ramps of the thrust sheets (Figs. 1, 8A and 8B) implies that the spatially homogenous uplift hypothesis underlying eq. 2 is only partially fulfilled. This may explain the small differences between predicted and measured divide migration celerity. However, over one order of magnitude of variation of the uplift rate, the divide migration velocities measured in series A experiments follow the values predicted by the approximation of eq. 2, within the 95% confidence envelop (Fig. 6). The divide migration velocities measured in series B experiments are also closely reproduced by eq. 2 within the range of standard deviation of the measured celerity.

2.5. Influence of the drainage network reorganization on the source areas and sedimentary fluxes: example from the experiment A2

Each one of the three captures observed in the experiment A2, above the thrust sheet n°4, involves an increase of the size of the upstream drainage area contributing to the channel ch2 (Fig. 8). Before the captures, its drainage area is only 20 cm² and it increases from 90 cm² after the first capture, to 800 cm² after the second and up to 1100 cm² after the third at $t = 450$ min. As a result, the size of the drainage area of channel ch2 increases by 55 folds its original size, while the drainage areas of adjacent channels ch1 and ch3 are divided by 2 and 20, respectively. A consequence of drainage reorganization triggered by divide migration and captures is a modification of the sediment routing system. Before the capture events, channels draining the entire accretionary prism feed the fans F1 and F3, and after captures they feed mainly the fan F2 and in minor proportion the fans F1 and F3.

Before the capture events, the headwaters of the captor channel ch2 migrate towards the inner part of the wedge (red profiles in Fig. 9A). After the first capture, a wave of incision propagates towards the inner part of the wedge (green profiles in the Fig. 9A), causing a sudden increase in the eroded volume and in the erosion rate of the captor channel (Figs. 9B and 9C).

To monitor sedimentation rate changes associated with drainage network reorganization we measure the thickness of sediments deposited before the captures and laying below the green layer of tinted material, and the thickness of the sediments deposited after the captures and laying above the first green layer (Fig. 10). Cross sections of fans F1, F2 and F3 fed by channels ch1, ch2 (captor channel) and ch3, respectively, are orientated perpendicular to the trace of the thrust sheet n°4 and pass through the apex of each fan.

From the areas of sediment accumulation measured in cross-sections between the base of the fans and the different tinted layers, we derive a 2D estimate of the mean sedimentation rates before and after the captures 1 and 2. Before the first capture the rates of sedimentation in the fans F1 and F3 (Δt_2 in Fig. 10) is 0.2 and 0.5 mm²/min respectively (Fig. 11). In the fan F2 fed by channel ch2 (future

captor) the sedimentation rate (Δt_2 in Fig. 10) is one order of magnitude lower, 0.01 mm²/min (Fig. 11). After the captures 1 and 2, the sedimentation rates in fans F1 and F3 ($\Delta t_3 + \Delta t_4$ in Fig. 10) decrease to 0.16 and 0.3 mm²/min, respectively (Fig. 11), i.e., about 20% and 40% of decrease in sedimentation rates, respectively. During the same interval the rate of sedimentation in the fan F2 ($\Delta t_3 + \Delta t_4$ in Fig. 10) increases to 0.4 mm²/min (Fig. 11), i.e. a 40 fold increase. This value is similar to the rates of sedimentation in the fans F1 and F3 before the capture events (Δt_2). Therefore, while the rate of sedimentation in the fan F2 is increasing the rate of sedimentation in the adjacent fans, F1 and F3, decreases. These results show that drainage reorganization can modify the sediment supply in front of an accretionary prism without any change in shortening rate or rainfall rate.

3. Discussion

3.1. Limitations of the models

Although rigorous mechanical and temporal scaling is not feasible for these types of experiments, at first order similarity criteria between models and nature in regard to dynamics, kinematics and geometry are respected, as well as the similarity in the erosion law. Then, morphodynamic analogue models are suitable to study geological processes that operate during hundreds of thousands to tens of millions of years, and at the scale of an alluvial fan up to a mountain range (Schumm *et al.*, 1987; Peakall *et al.*, 1996; Lague *et al.*, 2003; Babault *et al.*, 2005; Niemann & Hasbargen, 2005; Bonnet & Crave, 2006; Malverti *et al.*, 2008; Bonnet, 2009; Paola *et al.*, 2009; Graveleau *et al.*, 2011; Strak *et al.*, 2011; Graveleau *et al.*, 2015; Viaplana-Muzas *et al.*, 2015; Guerit *et al.*, 2016). In our experiments the length ratio L^* between models and nature ranges from 10^{-5} to 10^{-4} , 1 cm in the model is equivalent to hundreds of meters in nature, (Viaplana-Muzas *et al.*, 2015). The accretionary wedges we modelled would be equivalent to a mountain range of several tens of kilometers in length (strike) and width (dip). In the models, incision rates by persistent transverse channels range from ≈ 0.07 mm/min (I_{min_mod}) to ≈ 2 mm/min (I_{max_mod}) (Viaplana-Muzas *et al.*, 2015). Incision rates in rivers incising thrust sheets where rock uplift rate is slow as in the Middle Atlas of Morocco (Pastor *et al.*, 2015), or rapid as along the Main Frontal Thrust of the Himalaya (Lavé & Avouac, 2000) range between 0.3 mm/a (I_{min_nat}) and 15 mm/a (I_{max_nat}), respectively. Using these values and following Graveleau *et al.* (2011) and Strak *et al.* (2011), we deduce an incision rate ratio R_{mn}^* between models and nature ranging between 7×10^4 (I_{min_mod}/I_{min_nat}) and 1.2×10^5 (I_{max_mod}/I_{max_nat}). The celerity of divide migration in our models ranges from 0.2 mm/min to 3 mm/min (Fig. 6). Using R_{mn}^* , the equivalent rate of divide migration in nature would range between 8.6×10^{-4} m/a and 2.3×10^{-2} m/a. Analytical and numerical modeling predict divide migration rates in nature to range between 10^{-4} m/a and 10^{-3} m/a (Whipple *et al.*, 2017). Under spatially uniform rock uplift rate and rock erodibility, motion of a divide depends on the contrasts of erosion rates across a divide. In our models, incision rates are negligible in the hanging wall of the thrust sheets where the longitudinal channels have very low downstream slope. Then differential erosion is maximal across the divide enhancing divide migration rate, likely explaining the higher rates in our models. We consider that despite differences in model setup, our estimates agree with those of Whipple *et al.* (2017).

In the Central Range of the island of New Guinea, the rapidly eroding southern flank ($E_{max_CR} = 1.7$ mm/a) contrasts with the slowly eroding central high plateau ($E_{min_CR} < 0.7$ mm/a) (Weiland & Cloos, 1996), in a similar way as seen in our experiments. Considering the rate of differential erosion and the mean slope of the south flank, the main drainage divide would migrate toward the center of the Central Range at $\sim 10^{-2}$ m/a (Babault *et al.*, 2018). Using the minimum and maximum erosion rates in the Central Range to calculate the incision rate ratio R_{cr}^* , we obtain values ranging from 5×10^4 (I_{min_mod}/E_{min_CR}) to 6×10^5 (I_{max_mod}/E_{max_CR}) (very close to the R_{mn}^* ratio previously calculated using the Atlas of Morocco and Himalaya cases). Using R_{cr}^* , the equivalent divide migration rate would be $\simeq 2 \times 10^{-3}$ m/a. This value is five times smaller than that predicted for the Central Range ($\sim 10^{-2}$ m/a). Equation 2 shows that C_{pred} is an inverse function of mean channel downstream slope. In our experiments, channel downstream slopes are about two (0.2 m/m) to six (0.6 m/m) times higher than the mean slope of the southern flank of the Central Range (~ 0.09 m/m), which explains the difference in divide migration rates. The comparison to the drainage dynamics in the Central Range shows that differences in mean downstream channel slopes between our models and nature imply that divide migration rates may be underestimated by our physical models.

As underlined in other experimental modeling studies using similar setup and materials (e.g., Guerit *et al.*, 2016), model erosion is mainly driven by fluvial processes and slope processes (slope diffusion, landslides and sapping) being controlled by vertical and lateral channel erosion. We quantified the extent to which drainage divide migration is controlled by channel incision in equation 2. We obtained a C_{pred} close to, yet slightly smaller than ($\sim 10\%$), the mean measured celerity of divide migration (C_A) (Fig. 6). It means that the rate of divide migration is primarily controlled (90%) by channel incision. Because we ruled out the thrust sheets where erosion was driven by landslides, sapping may be responsible for this difference, therefore sapping would only accelerate divide migration rates by 10% in the models. Even if the contributing processes for divide migration in our models may not be fully similar to what occurs in nature, the similar divide migration rates between analytical/numerical models, natural examples, and our physical models support the applicability of our experimental results to study the effect of drainage network dynamics on erosion and sedimentation in nature.

3.2. Timing for captures to occur in the models

We only observe capture events in some of the thrust sheets of the three experiments run under the lowest shortening rate, and where longitudinal reaches have previously developed (A2, A3 and B1). We do not observe drainage reorganization in the experiments done at faster rates of shortening and dominated by larger longitudinal reaches (A4, A5, A6 and B2). In our experiments, a high threshold for erosion is imposed by material erodibility, resulting in the persistence of non-eroded areas on top of the thrust sheets where local slopes are too small for erosion to initiate. The successive accretion of new thrust sheets results in the back tilt of the older thrust sheets toward the inner part of the accretionary prism, inducing a decrease of the local slopes in their external limbs and the inhibition of erosion (Viaplana-Muzas *et al.*, 2015). Therefore the expansion of transverse channels in the experiments occurs only while a thrust sheet is active at the front of the

experimental prism and we refer to this time as the period of uplift and incision for that thrust. For a capture to occur, this period of time needs to be long enough for headwaters of the expanding transverse channels to reach the longitudinal channels; otherwise the tilt-induced inhibition of erosion freezes the onset of divide migration and drainage reorganization. We calculated the time needed for a capture to occur in the experiments, i.e., the drainage reorganization response time, dividing the distance between a longitudinal channel and the trace of a thrust, by the divide migration celerity measured in the experiments. In our experiments the spacing between thrust sheets is mostly independent from uplift rate (Viaplana-Muzas *et al.*, 2015) but we observe some variability (Figs. 3A, 4A and F and 5A and E). This variability is responsible for the different distances between a longitudinal channel and the trace of a thrust. These distances vary from 36 mm to 75 mm (mean is 54 mm \pm 11 mm, 1 σ), with values slightly higher in experiments run under higher uplift rate (A4, A5 and A6, B2).

Even if the drainage migration celerity increases with uplift rate, it does not compensate for the slight increase of distances between a longitudinal channel and the trace of a thrust with uplift rate. In the experiments in which captures occur (A2, A3 and B1), the duration of uplift and incision in the external limb of the thrust sheets equates or is higher than the time needed for a capture to occur (supplementary data Fig. SD4). In the other experiments (A4, A5, A6 and B2), the period of uplift and incision before the emergence of a new thrust sheet is too small for drainage reorganization to occur. Channel gradient decrease, below the threshold for erosion, and inhibition of erosion during back-tilting of the former thrust sheets when a new thrust sheet emerges, prevent transverse drainage expansion and reorganization to propagate into the inner part of the accretionary wedges.

3.3. Dynamics of drainage network during building of a fold-and-thrust belt

The experiments show that the longitudinal channels that developed in the early stages of thrust sheet emergence tend to disappear as they are uplifted at a higher elevation than their surroundings. Increasing incision rates in steep frontal transverse channels induce headward erosion and catchment expansion into the growing thrust sheets (Figs. 9A, 9B and 9C). As a result, drainage network reorganizes from longitudinal- to transverse-dominated through drainage divide migration and captures (Figs. 3, 4 and 5). Divide migration in our experiments is not linked to catchment shrinkage in response to tectonic shortening and shear deformation (e.g., Yang *et al.*, 2015), but is controlled by the increasing downstream slope and erosion rates of the expanding transverse rivers (Equation 2).

Drainage network evolution from longitudinal- to transverse-dominated is a dynamic process observable in some orogenic wedges submitted to very different shortening and precipitation rates, as the High Atlas of Morocco, the Andes and the Central Range of New Guinea (Babault *et al.*, 2012; Babault *et al.*, 2013; Babault *et al.*, 2018). In these mountain ranges, main divides propagate into the inner part of the orogenic wedges, and we can expect eventually a complete drainage reorganization to a more stable transverse-dominated drainage network, in which transverse catchments probably

reach a fixed geometry as proposed by Hovius (1996). Equation 2 gives a simple way to calculate from incision rates and mean slopes the velocity of divide migration into a slowly eroding and highly-elevated smooth erosional surface subjected to a constant uplift rate. This equation has been applied to the Central Range of New Guinea (Babault *et al.*, 2018). When corrected for a non-null erosion rate in the longitudinal-dominated drainage network, the mean celerity of divide migration (C_{pred}) in equation 2 becomes (Babault *et al.*, 2018):

$$C_{pred} = \frac{\Delta E}{\tan \theta} , \quad \text{eq. (6)}$$

C_{pred} depends on the mean differential erosion rate (ΔE) between the expanding transverse-dominated catchments and the shrinking longitudinal-dominated catchments, and the mean regional slope of the expanding catchments ($\tan \theta$). The mean differential erosion rate between the south flank of the Central Range of New Guinea and the inner Kemabu high plateau is >1 mm/a, and the mean regional slope of the south flank is $\theta = 5.7^\circ$ (Fig. 12). Assuming uniform rock uplift, equation 6 predicts a mean rate of divide migration $C_{pred} \geq 10^{-2}$ m/a in the Central Range of New Guinea. Given the uncertainties of incision rate ratios and differences in mean channel slopes, divide migration rates in our physical models are similar to those predicted for nature.

In our experimental study, hillslope processes may not be as important as they are in forcing divide migration in natural landscapes. In the Finisterre Range, a high plateau capped by karstified planar limestones is progressively removed (Hovius *et al.*, 1998). There, channel heads retreat and catchments expand by seepage-triggered landslides which are rooted at the base of the permeable limestones. It led Hovius (1998) to propose that during the initial stage of mountain building the mode and rate of drainage divide migration are governed by hillslope mass wasting, not by fluvial incision. In the western Central Range of the island of Papua New Guinea, the Kemabu plateau is also capped by limestones and seepage may also help failures to occur. However, like in other fold-and-thrust belts geologic contacts are seldom planar, and the role of seepage might be very limited in driving divide motion at the spatial scale of the Central Range, and by extension in any fold-thrust belts. A recent study shows that a minimum of 15% of divide migration is controlled by typhoon-triggered landslides in the Central Range of Taiwan (Dahlquist *et al.*, 2018). Other processes like earthquake-triggered landslides, a common process in tectonically active mountain belts, may increase this value. Landslides triggered by earthquakes or storms are also a dominant process of erosion in the steep hillslopes of the rapidly uplifting the Central Range of the island of Papua New Guinea which is subjected to heavy rainfalls (Simonett, 1967; Pain & F.Bowler, 1973; Keefer, 1994; Hovius *et al.*, 1998; Robbins & Petterson, 2015; Robbins, 2016), and it certainly contributes to divide mobility. All these types of landslide, triggered by different forcings, together probably govern drainage divide migration in active orogens. But it is generally accepted that landslides are coupled to the fluvial drainage network, which controls their occurrence and magnitude and their associated erosion rates and sediment fluxes (e.g., Burbank *et al.*, 1996; Montgomery, 2001; Montgomery & Brandon, 2002; Larsen & Montgomery, 2012). Then, over millions of years, i.e. at the timescale of fold-and-thrust belts growth, rates of divide migration are most likely controlled by fluvial erosion adjustment to rock uplift, i.e. to tectonics. Even if differences in hillslope processes exist between our analogue models and nature, drainage reorganization from early longitudinal rivers to transverse ones is most likely triggered by fluvial incision in natural landscapes, as in our models.

Lithologic variability in fold-thrust belts can influence the spatial and temporal pattern of erodibility and potentially influence landscape erosional response to external factors (e.g., Yanites *et al.*, 2017). In post-orogenic landscapes, where geologic contacts are horizontal or slightly dipping, spatial variations of substrate erodibility can alone trigger divide motion and river captures (Gallen, 2018). Numerical modeling also suggest that steady state divide position achieved in actively uplifting settings could even experience motions from one side to the opposite during exhumation of near planar harder layers (Forte & Whipple, 2018). Following these works, the rate of divide migration toward the interior of an accretionary wedge as described in our experiments may be modulated by lithologic variability. However, in the interior of an orogenic wedge, where the sedimentary cover has started to be removed by erosion and where horizontal contacts are minimal, the influence of lithology on divide motion may be of second order, tectonics being the main forcing (Forte & Whipple, 2018; Gallen, 2018). Hence, ongoing deformation should lead eventually to a reorganization from early longitudinal rivers to transverse ones, and rock-type related erodibility may only either temporally accelerate or delay drainage divide motion but probably not drainage reorganization pattern over millions of years. This is evidenced by the occurrence of such pattern of drainage reorganization in orogens with contrasting lithologies.

As the drainage network reorganization process from longitudinal- to transverse-dominated channels (i) is observed at all spatial scales (from model centimeters to nature kilometers scales), (ii) is mainly triggered by fluvial erosion, and (iii) occurs under steady shortening and precipitation rates, it can be considered as a generic process independent of any external forcing.

3.4. Implications of drainage dynamics on the sediment routing system

The varying sedimentary flux entering a foreland basin has traditionally been ascribed to tectonic pulses or climate variations. Ubiquitous and synchronous increases in sediment flux at global scale could be interpreted as a climatically-driven increase of erosion (Molnar & England, 1990; Molnar & Houseman, 2004). The corollary, a diachronous increase of sedimentation rate over a basin and a diachronous increase of erosion rate over an orogen, has been interpreted as evidence for sedimentation and erosion rate variations linked to tectonics such as thrusting (e.g., Charreau *et al.*, 2009). At the scale of an orogenic wedge, surface uplift related to thrust activity and crustal thickening is considered to result in increasing sediment accumulation in foreland basins during mountain building (Price, 1973; Beaumont, 1981; Puigdefàbregas & Souquet, 1986; Molnar & England, 1990; Jordan & Flemings, 1991; DeCelles & Giles, 1996; Kuhlemann *et al.*, 2002; Allen, 2008). Beside its control on sediment flux, the capacity of tectonics to control the drainage organization during mountain building implies that tectonics also controls the stratigraphic architecture in foreland basins (Heller *et al.*, 1988; Tucker & Slingerland, 1996; Gupta, 1997; Horton & DeCelles, 2001). In the case of a mountain front drained by transverse rivers, the high density of rivers that enter into a foreland basin leads to line-depositional systems. Conversely, the low density of transverse rivers in longitudinal-dominated drainage networks implies a limited number of outlets that feed the sedimentary basins and the routing system leads to point-source dispersal system pattern. These two end-member patterns of source-to-sink systems have been reproduced

experimentally (Viaplana-Muzas *et al.*, 2015). Here we show that under constant shortening and rainfall rates, tectonically-induced early drainage organization and later reorganization by captures decrease the spacing of outlets that feed a basin. These processes and the resulting changes also modify the contributing drainage areas, erosion rates and eventually local sedimentation rates at mountain outlets (Fig. 11). We show that an increase in upstream area results in an increase of the sedimentation rate in the captor outlet, while in the adjacent outlets the sedimentation rate decreases in response to upstream area loss (Fig. 11). Tectonics increases the potential energy for erosion in transverse channels, drainage divide migration and eventually capture, especially of longitudinal drainage. Hence, tectonics is responsible for capture-driven modulation of the sedimentary flux at the front of accretionary prisms.

In addition to modifying the sedimentation rate, drainage reorganization during mountain building should also influence the composition of the sediments and the grain size of the bed load that feed alluvial fans at mountain fronts. In the experiments, the material for erosion is spatially uniform so that changes in source area do not modify the composition and the grain size of the erosion products accumulated in the fans. In nature, a modification in drainage area is expected to result in different proportions of the eroded lithologies and in the consequent variable composition of erosion products, supporting an alternative explanation for provenance signals (e.g., Babault *et al.*, 2013; Babault *et al.*, 2018). Clastic grain size is also expected to be modified downstream of a capture point. A capture involves a sudden lowering of the base level in the captured channel, inducing a wave of erosion and the incision of a deep valley downstream of a knickpoint (e.g., Fig 9A). Landslide-derived boulders from the steep slopes of a valley are expected to increase the bed load grain size as seen in canyons that cut uplifting topographies (e.g., Whittaker *et al.*, 2010). On the other hand, the grain size in the fans fed by beheaded rivers is expected to decrease as the sediment transport capacity of rivers decreases (e.g., Maher *et al.*, 2007). Hence, the variation of sediment characteristics in foreland basin commonly used to infer sudden tectonic uplift or climate variations may lead to misinterpretations if its modulation by the drainage dynamics is not considered. The comparison of synchronous sedimentation variations in adjacent fans should serve as a diagnostic for a capture-driven origin. Inverse variation in sedimentary flux in adjacent fans, together with drastic change in clastic composition, is diagnostic of upstream capture. Finally, the intrinsic process of drainage reorganization during mountain building is ultimately expected to lead to a modification of the sedimentary architecture from point source dispersal system to line-depositional system.

4. Conclusions

The experiments show that in active fold-and-thrust belts divide migration and captures can occur under steady shortening and rainfall rate. These processes result in the reorganization of early drainage network inherited from thrust emergence, evolving from a longitudinal drainage to a transverse drainage, and in the drastic change of the size of drainage basins.

Experimental modeling shows that the rate of divide migration in transverse channel headwaters increases in a non-linear way with uplift rate. In the framework of the stream power erosion model, the experiments suggest that the exponent on the slope variable controls this non-linearity.

Experiments also show that under similar uplift rates, an increase of the rainfall rate results in an increase of the velocity of divide migration.

Under steady tectonic and climate conditions, drainage reorganization driven by the interactions between tectonics and erosion eventually modulates the distribution of sedimentary fluxes at the outlets of experimental wedges. We show that simultaneous and opposite variations in sedimentation rates in adjacent fans are a diagnostic criterion for drainage network reorganization in the source areas.

We propose that this sedimentary response to drainage reorganization is also recorded in foreland basins. In such settings, variations in sedimentation rates are usually attributed to variations of erosion in response to perturbation of tectonic uplift rate and/or climate. These interpretations assume that the drainage areas of the rivers entering a sedimentary basin do not change during mountain building. Modifications of catchment size in the source areas, as well as transport distances and slopes, triggered by the divide migration and capture processes, may additionally modify clastic sediment composition and sediment grain size.

Acknowledgments:

Financial support was provided to J. Babault by REPSOL, for M. Viaplana-Muzas PhD grant (PhD defended in 2015) and they also benefited from Spanish national projects (CGL2010-1516 and CONSOLIDER-Ingenio CSD2006-00041). We thank C. Romano from Géosciences Montpellier for technical assistance and we thank J. Malavieille for helpful discussions. Thanks to M. González, C. Díaz and E. Álvarez de Buergo for discussions on preliminary results of this work. We thank Chris Paola, Leonardo Cruz, Adam M. Forte and two anonymous reviewers for constructive reviews that greatly improved the manuscript, and the Associate Editor Nadine McQuarrie for her efforts.

5. References

- ALLEN, P.A. (2008) From Landscapes into Geological History. *Nature*, **451**, 274-276.
- ARMITAGE, J.J., DULLER, R.A., WHITTAKER, A.C. & ALLEN, P.A. (2011) Transformation of Tectonic and Climatic Signals from Source to Sedimentary Archive. *Nature Geoscience*, **4**, 231-235.
- BABAULT, J., BONNET, S., CRAVE, A. & VAN DEN DRIESSCHE, J. (2005) Influence of Piedmont Sedimentation on Erosion Dynamics of an Uplifting Landscape: An Experimental Approach. *Geology*, **33**, 301-304, doi: 310.1130/G21095.21091.
- BABAULT, J., VAN DEN DRIESSCHE, J. & TEIXELL, A. (2012) Longitudinal to Transverse Drainage Network Evolution in the High Atlas (Morocco): The Role of Tectonics. *Tectonics*, **31**, TC4020.
- BABAULT, J., TEIXELL, A., STRUTH, L., VAN DEN DRIESSCHE, J., ARBOLEYA, M.L. & TESÓN, E. (2013) Shortening, Structural Relief and Drainage Evolution in Inverted Rifts: Insights from the Atlas Mountains, the Eastern Cordillera of Colombia and the Pyrenees. *Geological Society, London, Special Publications*, **377**, 141-158.
- BABAULT, J., VIAPLANA-MUZAS, M., LEGRAND, X., VAN DEN DRIESSCHE, J., GONZÁLEZ-QUIJANO, M. & MUDD, S.M. (2018) Source-to-Sink Constraints on Tectonic and Sedimentary Evolution of the Western Central Range and Cenderawasih Bay (Indonesia). *Journal of Asian Earth Sciences*, **156**, 265-287.
- BEAUMONT, C. (1981) Foreland Basins. *Geophysical Journal of the Royal Astronomical Society*, **65**, 291-329.
- BISHOP, P. (1995) Drainage Rearrangement by River Capture, Beheading and Diversion. *Progress in Physical Geography*, **19**, 449-473.
- BONNET, S. & CRAVE, A. (2003) Landscape Response to Climate Change: Insights from Experimental Modeling and Implications for Tectonic Versus Climatic Uplift of Topography. *Geology*, **31**, 123-126.
- BONNET, S. & CRAVE, A. (2006) Macroscale Dynamics of Experimental Landscapes. *Geological Society, London, Special Publications*, **253**, 327-339.
- BONNET, S. (2009) Shrinking and Splitting of Drainage Basins in Orogenic Landscapes from the Migration of the Main Drainage Divide. *Nature Geoscience*, **2**, 897-897.
- BURBANK, MCLEAN, BULLEN, ABDRAKHMATOV & MILLER (1999) Partitioning of Intermontane Basins by Thrust-Related Folding, Tien Shan, Kyrgyzstan. *Basin Research*, **11**, 75-92.
- BURBANK, D.W., LELAND, J., FIELDING, E., ANDERSON, R.S., BROZOVIC, N., REID, M.R. & DUNCAN, C. (1996) Bedrock Incision, Rock Uplift and Threshold Hillslopes in the Northwestern Himalayas. *Nature*, **379**, 505-510.
- CASTELLTORT, S., GOREN, L., WILLETT, S.D., CHAMPAGNAC, J.-D., HERMAN, F. & BRAUN, J. (2012) River Drainage Patterns in the New Zealand Alps Primarily Controlled by Plate Tectonic Strain. *Nature Geoscience*, **5**, 744-748.
- CRAVE, A. & DAVY, P. (2001) A Stochastic "Precipiton" Model for Simulating Erosion/Sedimentation Dynamics. *Computers & Geosciences*, **27**, 815-827.

- CHARREAU, J., CHEN, Y., GILDER, S., BARRIER, L., DOMINGUEZ, S., AUGIER, R., SEN, S., AVOUAC, J.-P., GALLAUD, A., GRAVELEAU, F. & WANG, Q. (2009) Neogene Uplift of the Tian Shan Mountains Observed in the Magnetic Record of the Jingou River Section (Northwest China). *Tectonics*, **28**, TC2008.
- DAHLQUIST, M.P., WEST, A.J. & LI, G. (2018) Landslide-Driven Drainage Divide Migration. *Geology*, **46**, 403-406.
- DECELLES, P.G. & GILES, K.A. (1996) Foreland Basin Systems. *Basin Research*, **8**, 105-123.
- FORTE, A.M. & WHIPPLE, K.X. (2018) Criteria and Tools for Determining Drainage Divide Stability. *Earth and Planetary Science Letters*, **493**, 102-117.
- FOX, M., GOREN, L., MAY, D.A. & WILLETT, S.D. (2014) Inversion of Fluvial Channels for Paleorock Uplift Rates in Taiwan. *Journal of Geophysical Research: Earth Surface*, **119**, 1853-1875.
- GALLEN, S.F. (2018) Lithologic Controls on Landscape Dynamics and Aquatic Species Evolution in Post-Orogenic Mountains. *Earth and Planetary Science Letters*, **493**, 150-160.
- GOREN, L., WILLETT, S.D., HERMAN, F. & BRAUN, J. (2014) Coupled Numerical–Analytical Approach to Landscape Evolution Modeling. *Earth Surface Processes and Landforms*, **39**, 522-545.
- GRAVELEAU, F. & DOMINGUEZ, S. (2008) Analogue Modelling of the Interaction between Tectonics, Erosion and Sedimentation in Foreland Thrust Belts. *Comptes Rendus Geoscience*, **340**, 324-333.
- GRAVELEAU, F., HURTREZ, J.E., DOMINGUEZ, S. & MALAVIEILLE, J. (2011) A New Experimental Material for Modeling Relief Dynamics and Interactions between Tectonics and Surface Processes. *Tectonophysics*, **513**, 68-87.
- GRAVELEAU, F., MALAVIEILLE, J. & DOMINGUEZ, S. (2012) Experimental Modelling of Orogenic Wedges: A Review. *Tectonophysics*, **538–540**, 1-66.
- GRAVELEAU, F., STRAK, V., DOMINGUEZ, S., MALAVIEILLE, J., CHATTON, M., MANIGHETTI, I. & PETIT, C. (2015) Experimental Modelling of Tectonics–Erosion–Sedimentation Interactions in Compressional, Extensional, and Strike–Slip Settings. *Geomorphology*, **244**, 146-168.
- GUERIT, L., DOMINGUEZ, S., MALAVIEILLE, J. & CASTELLTORT, S. (2016) Deformation of an Experimental Drainage Network in Oblique Collision. *Tectonophysics*, **693**, 210-222.
- GUPTA, S. (1997) Himalayan Drainage Patterns and the Origin of Fluvial Megafans in the Ganges Foreland Basin. *Geology*, **25**, 11-14.
- HALLET, B. & MOLNAR, P. (2001) Distorted Drainage Basins as Markers of Crustal Strain East of the Himalaya. *Journal of Geophysical Research*, **106**, 13697-13709.
- HELLER, P.L., ANGEVINE, C.L., WINSLOW, N.S. & PAOLA, C. (1988) Two-Phase Stratigraphic Model of Foreland-Basin Sequences. *Geology*, **16**, 501-504.
- HORTON, B.K. & DECELLES, P.G. (2001) Modern and Ancient Fluvial Megafans in the Foreland Basin System of the Central Andes, Southern Bolivia: Implications for Drainage Network Evolution in Fold-Thrust Belts. *Basin Research*, **13**, 43-63.
- HUVIUS, N. (1996) Regular Spacing of Drainage Outlets from Linear Mountain Belts. *Basin Research*, **8**, 29-44.

- HOVIUS, N., STARK, C.P., TUTTON, M.A. & ABBOTT, L.D. (1998) Landslide-Driven Drainage Network Evolution in a Pre-Steady-State Mountain Belt: Finisterre Mountains, Papua New Guinea. *Geology*, **26**, 1071-1074.
- HOWARD, A.D. (1967) Drainage Analysis in Geologic Interpretation: A Summation. *AAPG bulletin*, **51**, 2246-2259.
- HOWARD, A.D. & KERBY, G. (1983) Channel Changes in Badlands. *Geological Society of America Bulletin*, **94**, 739-752.
- JACKSON, J., NORRIS, R., YOUNGSON, J. & WOJTAL, S.F. (1996) The Structural Evolution of Active Fault and Fold Systems in Central Otago, New Zealand; Evidence Revealed by Drainage Patterns. *Journal of Structural Geology*, **18**, 217-234.
- JORDAN, T.E. & FLEMINGS, P.B. (1991) Large-Scale Stratigraphic Architecture, Eustatic Variation, and Unsteady Tectonism: A Theoretical Evaluation. *Journal of Geophysical Research*, **96**, 6681-6699.
- KEEFER, D.K. (1994) The Importance of Earthquake-Induced Landslides to Long-Term Slope Erosion and Slope-Failure Hazards in Seismically Active Regions. *Geomorphology*, **10**, 265-284.
- KENDRICK, R.D. (2000) Structure, Tectonics and Thermochronology of the Irian Jaya Fold Belt, Irian Jaya, Indonesia. PhD. Thesis, La Trobe University, Victoria, Australia.
- KUHLEMANN, FRISCH, SZÉKELY, DUNKL & KÁZMÉR (2002) Post-Collisional Sediment Budget History of the Alps: Tectonic Versus Climatic Control. *International Journal of Earth Sciences*, **91**, 818-837.
- LAGUE, D., CRAVE, A. & DAVY, P. (2003) Laboratory Experiments Simulating the Geomorphic Response to Tectonic Uplift. *Journal of Geophysical Research*, **108**, ETG 3-1–ETG 3-20, 2008.
- LAGUE, D. (2014) The Stream Power River Incision Model: Evidence, Theory and Beyond. *Earth Surface Processes and Landforms*, **39**, 38-61.
- LARSEN, I.J. & MONTGOMERY, D.R. (2012) Landslide Erosion Coupled to Tectonics and River Incision. *Nature Geoscience*, **5**, 468-473.
- LAVÉ, J. & AVOUAC, J.P. (2000) Active Folding of Fluvial Terraces across the Siwaliks Hills, Himalayas of Central Nepal. *Journal of Geophysical Research-Solid Earth*, **105**, 5735-5770.
- LEEDER, M. (1997) Sedimentary Basins: Tectonic Recorders of Sediment Discharge from Drainage Catchments. *Earth Surface Processes and Landforms*, **22**, 229-237.
- LEEDER, M.R., HARRIS, T. & KIRKBY, M.J. (1998) Sediment Supply and Climate Change: Implications for Basin Stratigraphy. *Basin research*, **10**, 7-18.
- MAHER, E., HARVEY, A.M. & FRANCE, D. (2007) The Impact of a Major Quaternary River Capture on the Alluvial Sediments of a Beheaded River System, the Rio Alias Se Spain. *Geomorphology*, **84**, 344-356.
- MALVERTI, L., LAJEUNESSE, E. & MÉTIVIER, F. (2008) Small Is Beautiful: Upscaling from Microscale Laminar to Natural Turbulent Rivers. *Journal of Geophysical Research: Earth Surface*, **113**, F04004.
- MEADE, R.H. (1982) Sources, Sinks, and Storage of River Sediment in the Atlantic Drainage of the United States. *The Journal of Geology*, **90**, 235-252.

- MOLNAR, P. & ENGLAND, P. (1990) Late Cenozoic Uplift of Mountain Ranges and Global Climate Change: Chicken or Egg? *Nature*, **346**, 29-34.
- MOLNAR, P. & HOUSEMAN, G.A. (2004) The Effects of Buoyant Crust on the Gravitational Instability of Thickened Mantle Lithosphere at Zones of Intracontinental Convergence. *Geophysical Journal International*, **158**, 1134-1150.
- MONTGOMERY, D.R. (2001) Slope Distributions, Threshold Hillslopes, and Steady-State Topography. *American-Journal-of-Science*, **301**, 432-454.
- MONTGOMERY, D.R. & BRANDON, M.T. (2002) Topographic Controls on Erosion Rates in Tectonically Active Mountain Ranges. *Earth and Planetary Science Letters*, **201**, 481-489.
- NIEMANN, J.D. & HASBARGEN, L.E. (2005) A Comparison of Experimental and Natural Drainage Basin Morphology across a Range of Scales. *Journal of Geophysical Research*, **110**, F04017.
- PAIN, C.F. & F.BOWLER, J.M. (1973) Denudation Following the November 1970 Earthquake at Madang, Papua New Guinea. *Zeitschrift fuer Geomorphologie*, **18**, 92-104.
- PAOLA, C., STRAUB, K., MOHRIG, D. & REINHARDT, L. (2009) The "Unreasonable Effectiveness" of Stratigraphic and Geomorphic Experiments. *Earth-Science Reviews*, **97**, 1-43.
- PASTOR, A., BABAUT, J., OWEN, L.A., TEIXELL, A. & ARBOLEYA, M.-L. (2015) Extracting Dynamic Topography from River Profiles and Cosmogenic Nuclide Geochronology in the Middle Atlas and the High Plateaus of Morocco. *Tectonophysics*, **663**, 95-109.
- PEAKALL, J., ASHWORTH, P.J. & BEST, J.L. (1996) Physical Modelling in Fluvial Geomorphology: Principles, Applications and Unresolved Issues. In: *The Scientific Nature of Geomorphology* (Ed. by B. L. Rhoads & C. E. Thorn), Wiley & Sons, Chichester, 221-253.
- PEIZHEN, Z., MOLNAR, P. & DOWNS, W.R. (2001) Increased Sedimentation Rates and Grain Sizes 2-4 Myr Ago Due to the Influence of Climate Change on Erosion Rates. *Nature*, **410**, 891-897.
- PELLETIER, J.D. (2004) Persistent Drainage Migration in a Numerical Landscape Evolution Model. *Geophysical Research Letters*, **31**, L20501.
- PERRON, J.T., RICHARDSON, P.W., FERRIER, K.L. & LAPOTRE, M. (2012) The Root of Branching River Networks. *Nature*, **492**, 100-103.
- PRICE, R.A. (1973) Large Scale Gravitational Flow of Supracrustal Rocks, Southern Canadian Rockies. In: *Gravity and tectonics* (Ed. by K. A. Dejong & R. Scholten), pp. 491-502. John Wiley and sons, New York.
- PUIGDEFÀBREGAS, C. & SOUQUET, P. (1986) Tectono-Sedimentary Cycles and Depositional Sequences of the Mesozoic and Tertiary from the Pyrenees. *Tectonophysics*, **129**, 173-204.
- ROBBINS, J.C. & PETERSON, M.G. (2015) Landslide Inventory Development in a Data Sparse Region: Spatial and Temporal Characteristics of Landslides in Papua New Guinea. *Natural Hazards and Earth System Sciences Discussion*, **3**, 4871-4917.
- ROBBINS, J.C. (2016) A Probabilistic Approach for Assessing Landslide-Triggering Event Rainfall in Papua New Guinea, Using Trmm Satellite Precipitation Estimates. *Journal of Hydrology*, **541**, 296-309.
- SCHUMM, S.A., MOSLEY, M.P. & WEAVER, W.E. (1987) *Experimental Fluvial Geomorphology*. John Wiley & Sons, New York, NY, United States.

- SIMONETT, D.S. (1967) Landslide Distribution and Earthquakes in the Bewani and Torricelli Mountains, New Guinea: A Statistical Analysis. In: *Landform Studies from Australia and New Guinea* (Ed. by J. N. Jennings & J. A. Mabbutt), Cambridge Univ. Press, Cambridge, 64-84.
- SNYDER, N.P., WHIPPLE, K.X., TUCKER, G.E. & MERRITTS, D.J. (2000) Landscape Response to Tectonic Forcing: Digital Elevation Model Analysis of Stream Profiles in the Mendocino Triple Junction Region, Northern California. *Geological Society of America Bulletin*, **112**, 1250-1263.
- STRAK, V., DOMINGUEZ, S., PETIT, C., MEYER, B. & LOGET, N. (2011) Interaction between Normal Fault Slip and Erosion on Relief Evolution: Insights from Experimental Modelling. *Tectonophysics*, **513**, 1-19.
- TALLING, P.J., STEWART, M.D., STARK, C.P., GUPTA, S. & VINCENT, S.J. (1997) Regular Spacing of Drainage Outlets from Linear Fault Blocks. *Basin Research*, **9**, 275-302.
- TOMKIN, J.H. & BRAUN, J. (1999) Simple Models of Drainage Reorganisation on a Tectonically Active Ridge System. *New Zealand Journal of Geology and Geophysics*, **42**, 1-10.
- TUCKER, G.E. & SLINGERLAND, R. (1994) Erosional Dynamics, Flexural Isostasy, and Long-Lived Escarpments: A Numerical Modeling Study. *Journal of Geophysical Research*, **99**, 12,229-212,243.
- TUCKER, G.E. & SLINGERLAND, R. (1996) Predicting Sediment Flux from Fold and Thrust Belts. *Basin research*, **8**, 329-349.
- UEDA, K., WILLETT, S.D., GERYA, T. & RUH, J. (2015) Geomorphological–Thermo-Mechanical Modeling: Application to Orogenic Wedge Dynamics. *Tectonophysics*, **659**, 12-30.
- VAN DER BEEK, P., CHAMPEL, B. & MUGNIER, J.-L. (2002) Control of Detachment Dip on Drainage Development in Regions of Active Fault-Propagation Folding. *Geology*, **30**, 471-474.
- VIAPLANA-MUZAS, M., BABAUT, J., DOMINGUEZ, S., VAN DEN DRIESSCHE, J. & LEGRAND, X. (2015) Drainage Network Evolution and Patterns of Sedimentation in an Experimental Wedge. *Tectonophysics*, **664**, 109-124.
- WEILAND, R.J. & CLOOS, M. (1996) Pliocene–Pleistocene Asymmetric Unroofing of the Irian Fold Belt, Irian Jaya, Indonesia: Apatite Fission-Track Thermochronology. *Geological Society of America Bulletin*, **108**, 1438-1449.
- WHIPPLE, K.X. & TUCKER, G.E. (1999) Dynamics of the Stream-Power River Incision Model: Implications for Height Limits of Mountain Ranges, Landscape Response Timescales, and Research Needs. *Journal of Geophysical Research*, **104**, 17,661-617,674.
- WHIPPLE, K.X. (2001) Fluvial Landscape Response Time: How Plausible Is Steady-State Denudation? *American Journal of Science*, **301**, 313-325.
- WHIPPLE, K.X., FORTE, A.M., DIBIASE, R.A., GASPARINI, N.M. & OUIMET, W.B. (2017) Timescales of Landscape Response to Divide Migration and Drainage Capture: Implications for the Role of Divide Mobility in Landscape Evolution. *Journal of Geophysical Research: Earth Surface*, **122**, 248-273.
- WHITTAKER, A.C., COWIE, P.A., ATTAL, M., TUCKER, G.E. & ROBERTS, G.P. (2007) Bedrock Channel Adjustment to Tectonic Forcing: Implications for Predicting River Incision Rates. *Geology*, **35**, 103-106.

WHITTAKER, A.C., ATTAL, M. & ALLEN, P.A. (2010) Characterising the Origin, Nature and Fate of Sediment Exported from Catchments Perturbed by Active Tectonics. *Basin Research*, **22**, 809-828.

WILLETT, S.D., SLINGERLAND, R. & HOVIUS, N. (2001) Uplift, Shortening, and Steady State Topography in Active Mountain Belts. *American Journal of Science*, **301**, 455-485.

WILLETT, S.D., MCCOY, S.W., PERRON, J.T., GOREN, L. & CHEN, C.-Y. (2014) Dynamic Reorganization of River Basins. *Science*, **343**, 12487650-12487659.

YANG, R., WILLETT, S.D. & GOREN, L. (2015) In Situ Low-Relief Landscape Formation as a Result of River Network Disruption. *Nature*, **520**, 526-529.

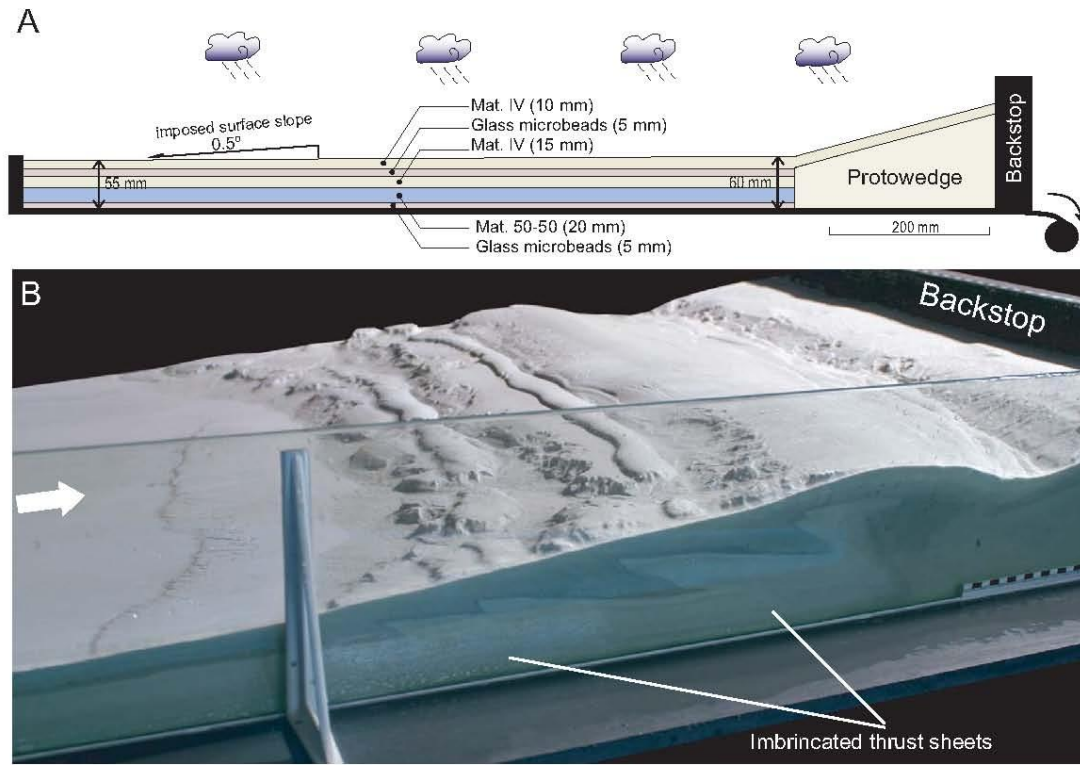
YANITES, B.J., BECKER, J.K., MADRITSCH, H., SCHNELLMANN, M. & EHLERS, T.A. (2017) Lithologic Effects on Landscape Response to Base Level Changes: A Modeling Study in the Context of the Eastern Jura Mountains, Switzerland. *Journal of Geophysical Research: Earth Surface*, **122**, 2196-2222.

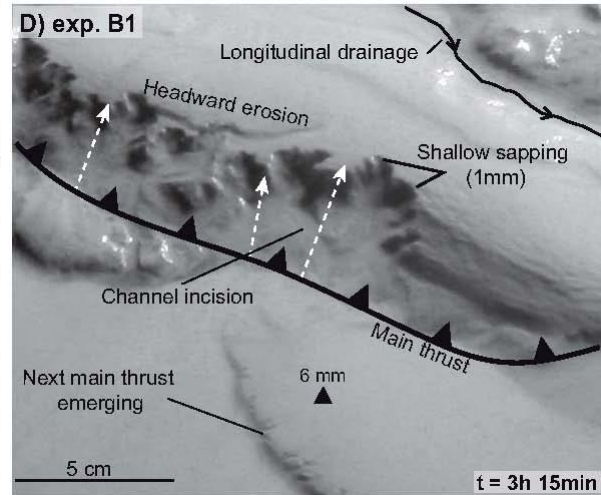
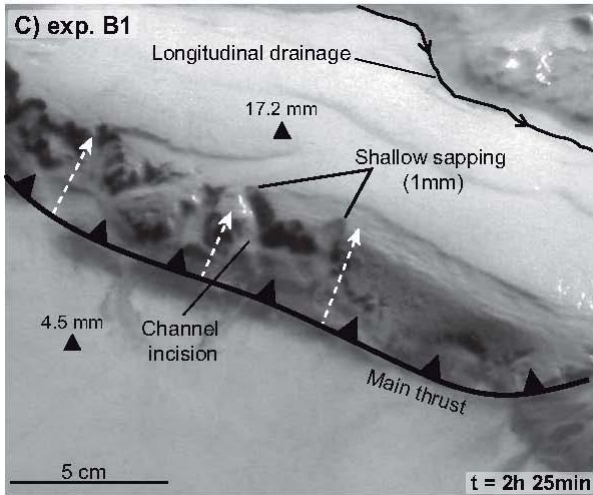
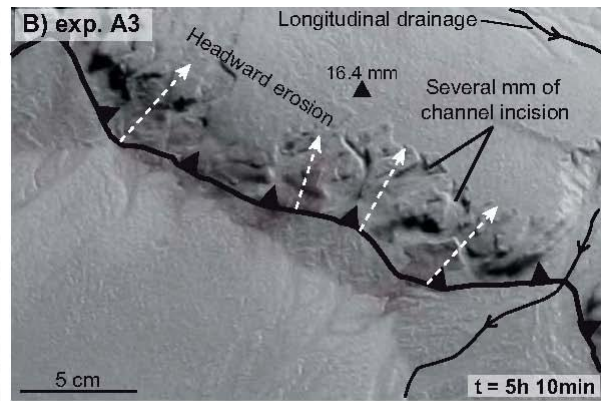
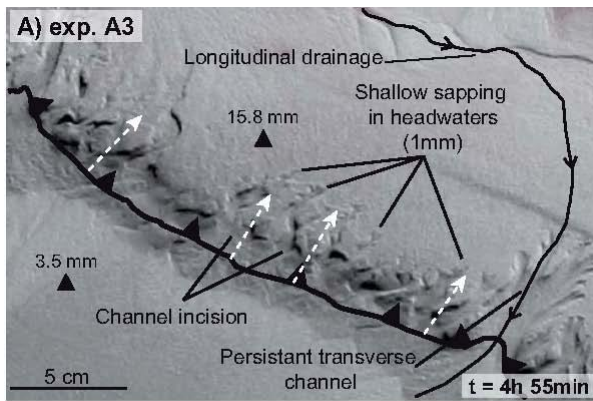
Table 1. Boundary conditions of the experimental thrust wedges analyzed in this work.

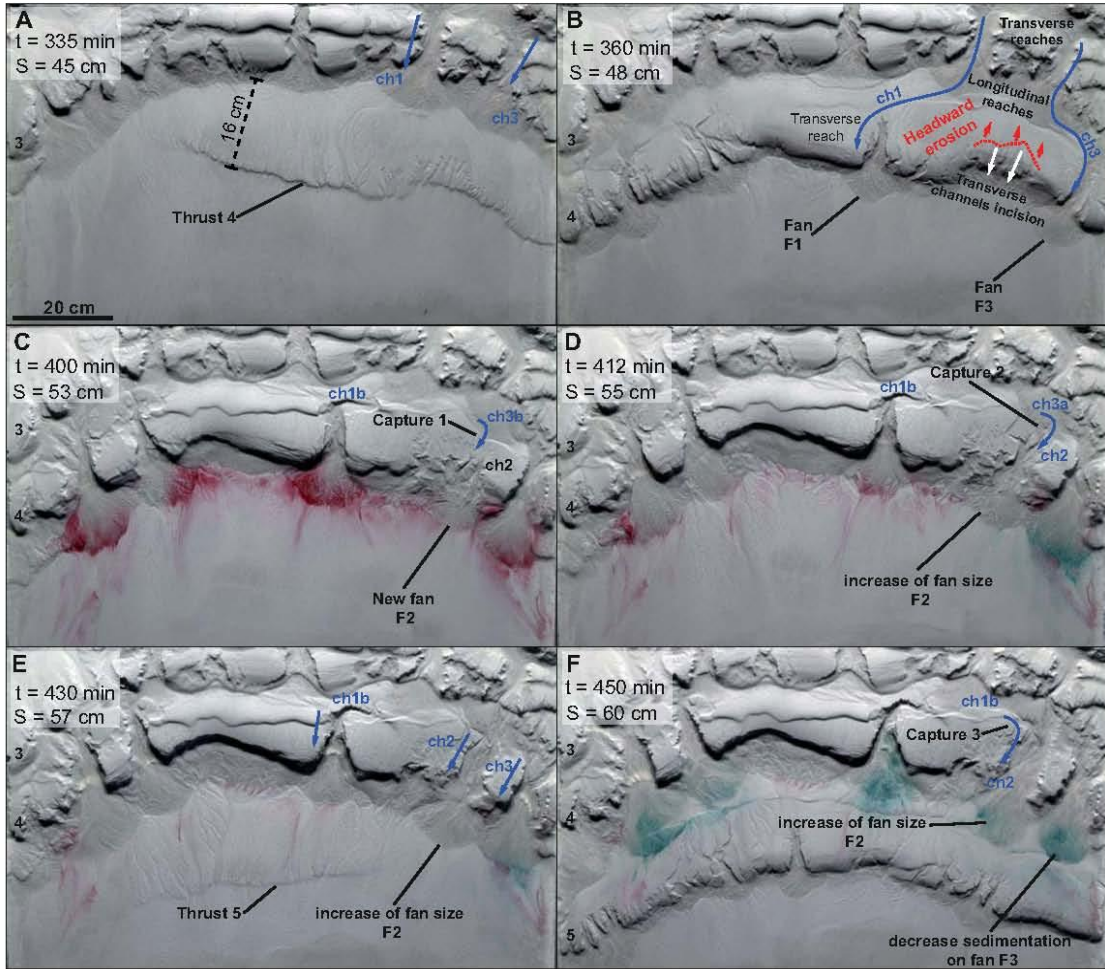
Experiment	Rainfall rate (mm/h)	Shortening rate (cm/h)	Shortening * (cm)	Thrust sheets*	Numbering of the thrust sheets [†]
A2	9	8	60	5	2, 3 and 4
A3	9	9	91	8	2,3 and 4
A4	Series A	20	94	7	2 and 3
A5	9	50	96	8	3, 4 and 6
A6	9	100	95	7	3 and 4
B1	Series B	8	55	5	3 and 4
B2	18	18	57	5	2, 3 and 4

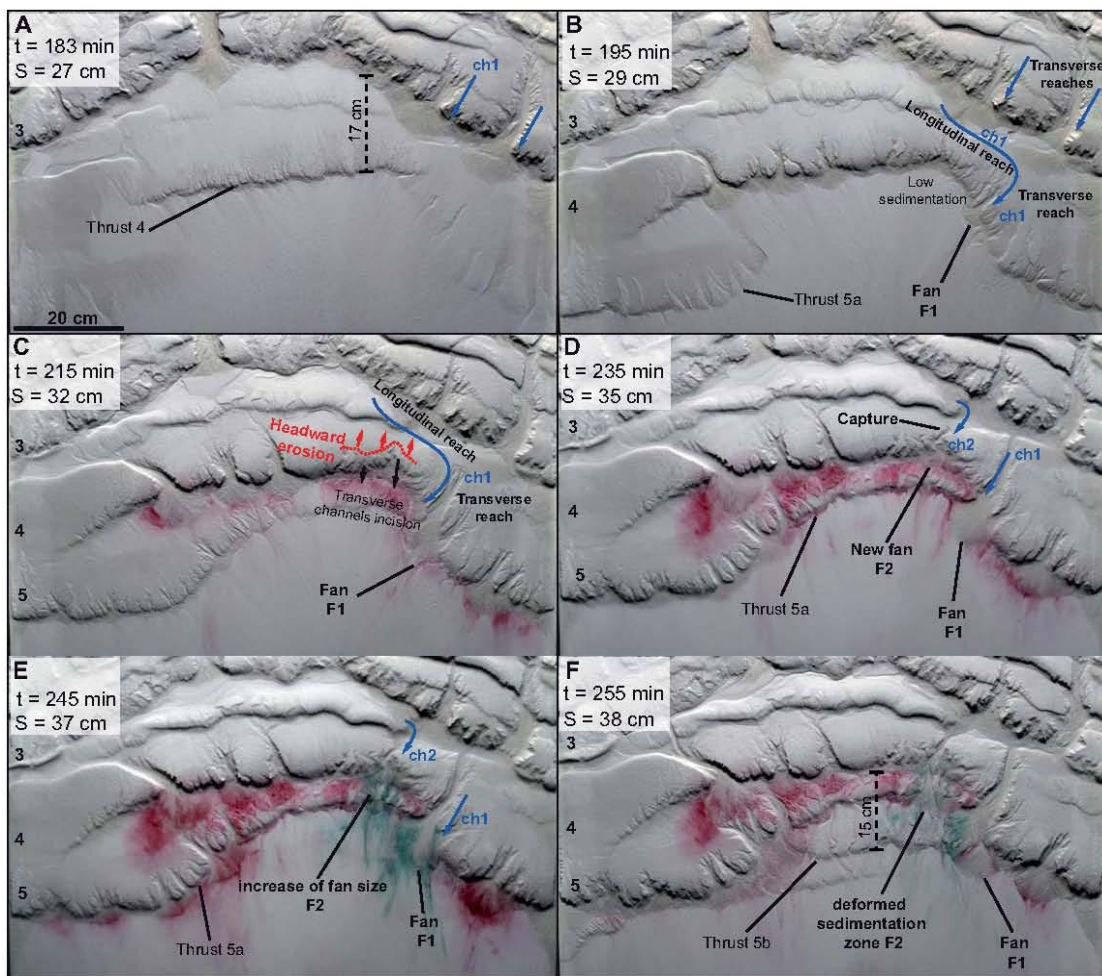
* Counted at the end of the experiments

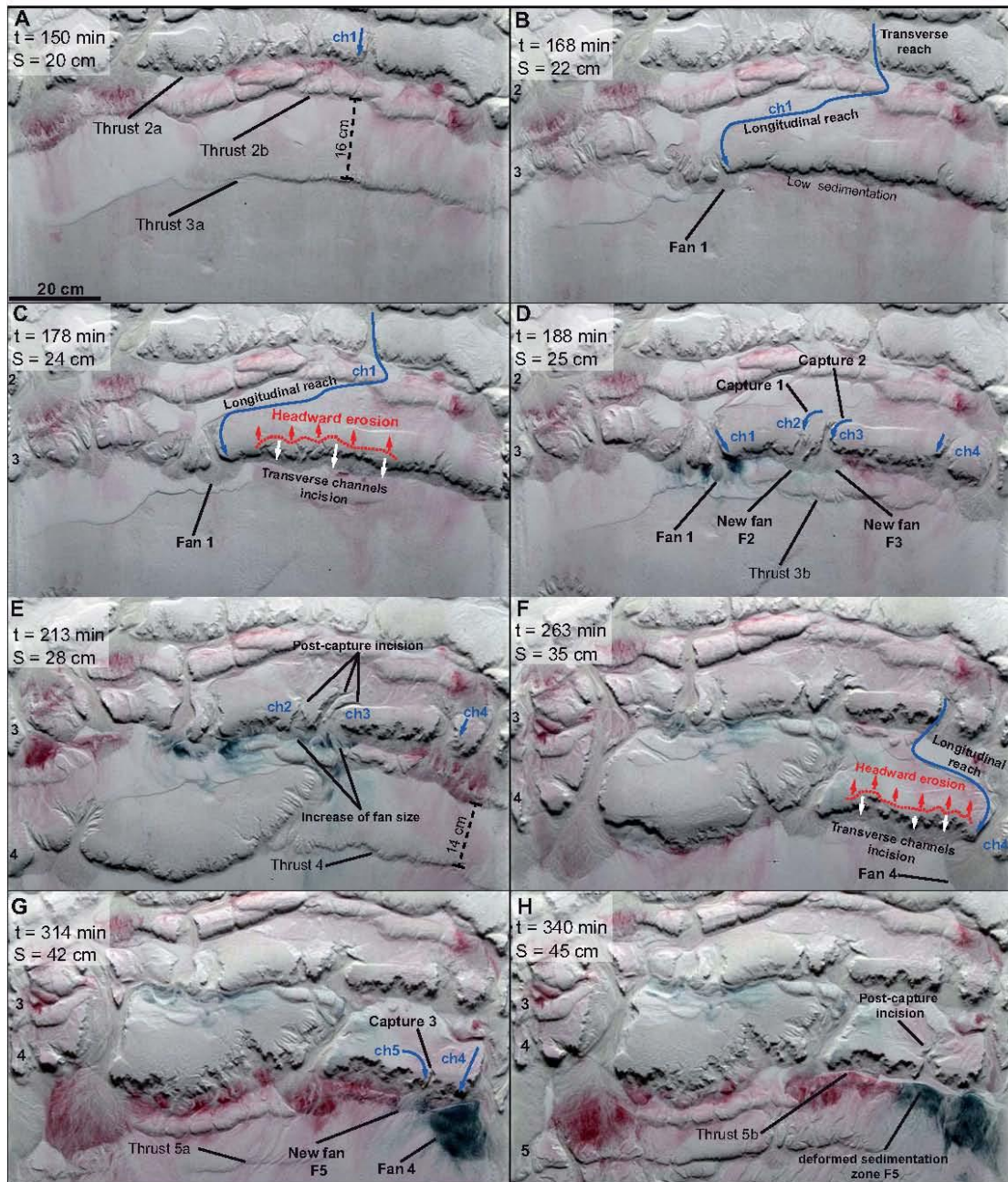
[†] Analyzed in this work

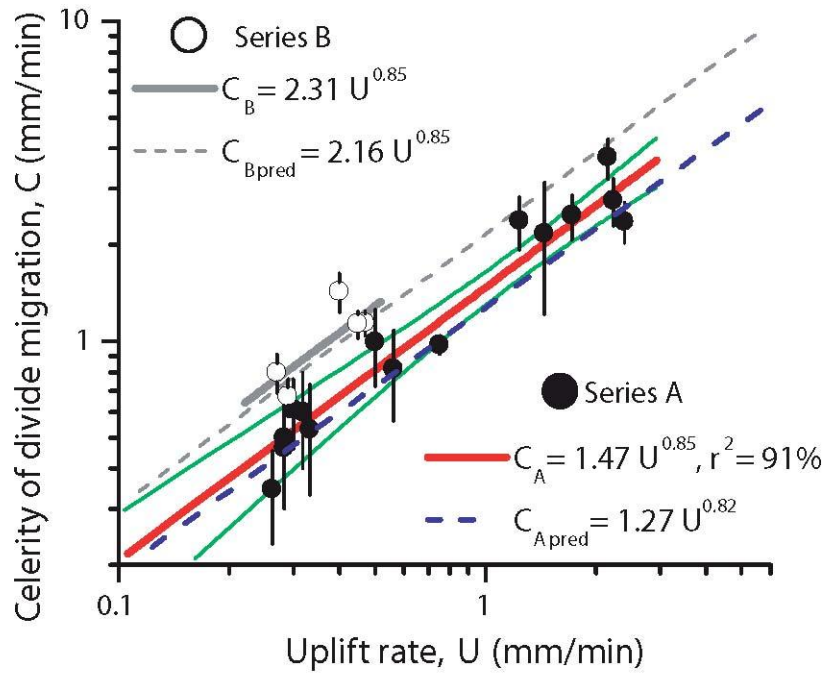


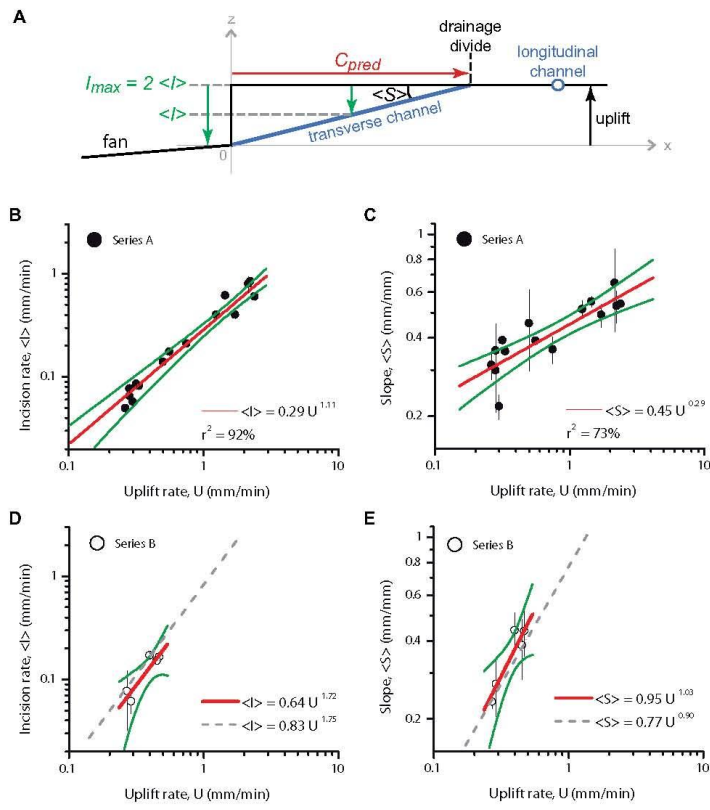




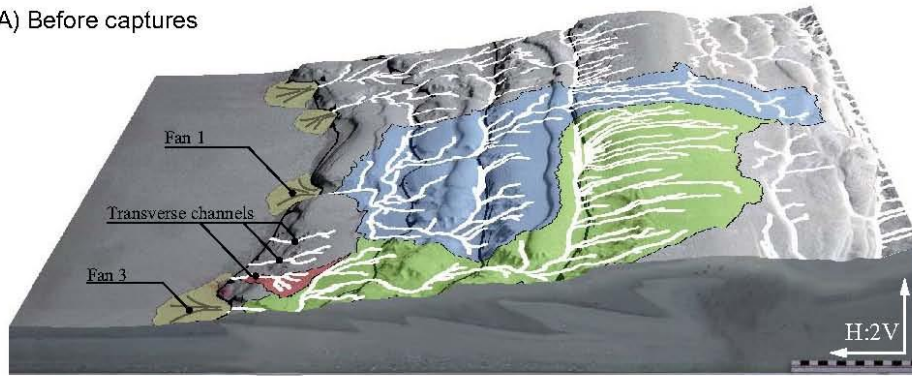








A) Before captures



B) After captures

